Afr. Mat. (2016) 27:1111–1137
DOI 10.1007/s13370-016-0399-y

CrossMark

Linear and weakly nonlinear magnetoconvection in a porous medium with a thermal nonequilibrium model

I. S. Shivakumara[1] · **A. L. Mamatha**[2] · **M. Ravisha**[3]

Received: 21 September 2014 / Accepted: 28 January 2016 / Published online: 1 March 2016

Abstract Two-dimensional magnetoconvection in a layer of Brinkman porous medium with local thermal nonequilibrium (LTNE) model is investigated by performing both linear and weakly nonlinear stability analyses. Condition for the occurrence of stationary and oscillatory convection is obtained in the case of linear stability analysis. It is observed that the presence of magnetic field is to introduce oscillatory convection once the Chandrasekhar number exceeds a threshold value if the ratio of the magnetic diffusivity to the thermal diffusivity is sufficiently small. Besides, asymptotic solutions for both small and large values of the inter-phase heat transfer coefficient are presented for the steady case. A weakly nonlinear stability analysis is performed by constructing a system of nonlinear autonomous ordinary differential equations. It is observed that subcritical steady convection is possible for certain choices of physical parameters. Heat transport is calculated in terms of Nusselt number. Increasing the value of Chandrasekhar number, inter-phase heat transfer coefficient and the inverse Darcy number is to decrease the heat transport, while increasing the ratio of the magnetic diffusivity to the thermal diffusivity and the porosity modified conductivity ratio shows an opposite kind of behavior on the heat transfer.

Keywords Convection · Local thermal nonequilibrium · Magnetic field · Porous medium

✉ I. S. Shivakumara
iskumar2006@gmail.com; shivakumarais@gmail.com

A. L. Mamatha
mamatharavisha@gmail.com

M. Ravisha
ravishmamatha@gmail.com

[1] Department of Mathematics, UGC-Centre for Advanced Studies in Fluid Mechanics, Bangalore University, Bangalore 560 001, India

[2] Department of Mathematics, Smt. Rukmini Shedthi Memorial National Government First Grade College, Barkur 576210, India

[3] Department of Mathematics, Dr. G. Shankar Government Women's First Grade College and Post Graduate Study Centre, Ajjarakadu, Udupi 576101, India

Mathematics Subject Classification 80A

1 Introduction

Thermal convective instability in an electrically conducting horizontal fluid layer in the presence of a uniform magnetic field, known as magnetoconvection, has been studied extensively by many authors (Thompson [1], Chandrasekhar [2], Busse [3], Rudraiah, [4], Weiss [5,6], Knobloch et al. [7], Proctor and Weiss [8]). Recently, Harfash and Straughan [9] have studied the effect of vertical magnetic field on convective movement of a reacting solute in a viscous incompressible fluid occupying a plane layer. The thresholds for linear instability are found and compared with those derived by a global nonlinear energy stability analysis. In somewhat seemingly related study, Makinde [10] and Makinde and Mhone [11] have limited their investigations to analyze the stability of magneto-hydrodynamic plane-Poiseuille and Jeffery–Hamel flows, respectively.

Nonetheless, magnetoconvection in a porous medium has received limited attention despite its importance and relevance in many engineering applications and in geophysics to study the Earth's core and to understand the performance of petroleum reservoir (Wallace et al. [12]). There are few investigations concerning the problem of thermal convection in an electrically conducting fluid-saturated porous medium in the presence of a uniform vertical magnetic field (Rudraiah [13], Rudraiah and Vortmeyer [14], Rudraiah [15], Raptis and Vlahos [16], Raptis and Tzivanidis [17], Takhar and Ram [18]). Bergman and Fearn [19] have explained convection in a mushy layer, often assumed to be an active porous layer with Newtonian fluids, at the Earth's inner–outer core boundary in the presence of a magnetic field. They have concluded that the magnetic field may be strong enough to act against the tendency for convection to be in the form of chimneys.

A systematic study on the stability of an electrically conducting fluid saturating a porous medium in the presence of a uniform magnetic field using Brinkman model is considered by Alchaar et al. [20] for rigid-rigid, free-free and rigid-free boundaries by considering constant-flux thermal boundary conditions. Bergman et al. [21] have provided experimental evidence that the presence of a magnetic field can significantly reduce the chimney formation in a mushy layer. They have conducted experiments for several values of the mush Rayleigh number including ones not far from onset of motion in a mushy layer subjected to a horizontal magnetic field. Bhadauria [22] has discussed the effect of temperature modulation on the onset of thermal convection in an electrically conducting fluid-saturated porous medium subjected to a vertical magnetic field. An investigation is conducted to analyze the marginal stability with and without magnetic field in a mushy layer by Muddamallappa et al. [23]. The effects of Chandrasekhar number and Robert number are analyzed on the problem. Bhatta et al. [24] have studied steady magnetoconvection in a horizontal mushy layer. Nield [25] has expressed the impracticality of MHD convection as there are no experimental papers on this topic, while Riahi [26] has clarified this point and cited some experimental works concerning the study.

The previous studies on magnetoconvection in a porous medium are based on traditional local thermal equilibrium (LTE) model; that is, the macroscopic temperatures of the fluid and solid phases of the porous medium are close enough so that a single temperature equation is used to describe the heat transport process. However, this assumption is not valid for some applications where a substantial temperature difference exists between the solid phase and the fluid phase. Then separate heat transport equations for solid and fluid phases of the porous medium are used and such macroscopic model is referred to as local thermal nonequilibrium (LTNE) model. Such a model tends to become more and more popular in

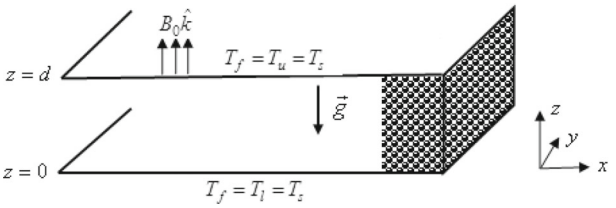

Fig. 1 Physical configuration

the study of heat transfer problems in porous media as the situations encountered in many naturally occurring phenomena and also in many engineering applications involve large thermal constraints (Alzami and Vafai [27], Straughan [28], Malashetty et al. [29], Nield and Bejan [30] and references therein). Under the circumstances, consideration of LTNE model in the study of linear and nonlinear thermal convective instability in porous media is warranted as propounded by many researchers. Srivastava et al. [31] have investigated the onset of thermal convection in an electrically conducting fluid-saturated anisotropic Darcy porous medium when the fluid and solid phases are in LTNE. Shivakumara et al. [32,33] have used LTNE model to investigate ferromagnetic convection in a layer of porous medium in the presence of a uniform vertical magnetic field.

The modeling of non-Darcian transport through porous media with LTNE model has been the subject of various recent studies due to the increasing need for a better understanding of the associated transport processes. Such a study involving electrically conducting fluids in the presence of a uniform magnetic field has not received due attention in the literature despite its importance in geophysics and solidification processes encountered in various fields. The intent of the present paper is to study both linear and weakly nonlinear magnetoconvection in a layer of Brinkman porous medium by considering a two-field temperature model for energy equation. To study nonlinear stability analysis, a truncated model is introduced to construct a system of autonomous nonlinear ordinary differential equations with the properties that the linear theory and the finite amplitude solutions obtained up to second order in the amplitude expansion, are identical to those obtained in the case of full problem. It is observed that subcritical motions are possible for a suitable choice of physical parameters. The heat transport is calculated in terms of Nusselt number.

2 Formulation of the problem

The physical configuration is as shown in Fig. 1. We consider an incompressible electrically conducting fluid-saturated horizontal layer of Brinkman porous medium of thickness d. A Cartesian coordinate system (x, y, z) is chosen such that the origin is at the bottom of the porous layer and the z-axis is directed vertically upward. Gravity acts in the negative z-direction and a uniform applied magnetic field of magnitude B_0 is acting in the vertical direction. The lower and upper surfaces of the porous layer are held fixed at constant temperatures T_l and T_u $(< T_l)$, respectively. The solid and fluid phases of the porous medium are considered to be in LTNE and a two-field model for temperatures is used. It is also assumed that the solid and fluid phases have identical temperatures at the bounding surfaces of porous layer.

The basic equations are:

$$\nabla . \vec{q} = 0 \tag{1}$$

$$\rho_0 \left[\frac{1}{\varepsilon}\frac{\partial \vec{q}}{\partial t} + \frac{1}{\varepsilon^2}(\vec{q}\cdot\nabla)\vec{q}\right] = -\nabla P + \rho_f \vec{g} + \frac{1}{\mu_m}(\vec{B}\cdot\nabla)\vec{B} - \frac{\mu_f}{K}\vec{q} + \tilde{\mu}_f \nabla^2 \vec{q} \quad (2)$$

$$\nabla . \vec{B} = 0 \quad (3)$$

$$\varepsilon \frac{\partial \vec{B}}{\partial t} = \nabla \times (\vec{q} \times \vec{B}) + \nu_{me} \nabla^2 \vec{B} \quad (4)$$

$$\varepsilon (\rho_0 c_p)_f \frac{\partial T_f}{\partial t} + (\rho_0 c_p)_f (\vec{q}\cdot\nabla) T_f = \varepsilon k_f \nabla^2 T_f + h(T_s - T_f) \quad (5)$$

$$(1-\varepsilon)(\rho_0 c)_s \frac{\partial T_s}{\partial t} = (1-\varepsilon) k_s \nabla^2 T_s - h(T_s - T_f) \quad (6)$$

$$\rho_f = \rho_0 \left\{1 - \beta(T_f - T_l)\right\} \quad (7)$$

where $\vec{q}$ the seepage velocity vector, (u, v, w), T_f the temperature of the fluid, T_s the temperature of the solid, $\vec{B}$ the magnetic induction field, P the total pressure, $\vec{g}$ the gravitational acceleration, ρ_f the fluid density, ρ_0 the reference density, μ_f the dynamic viscosity, $\tilde{\mu}_f$ the effective viscosity, μ_m the magnetic permeability, ε the porosity of the medium, K the permeability of the porous medium, c the specific heat of the solid, $c_p$the specific heat of the fluid at constant pressure of the fluid, h the inter-phase heat transfer coefficient, ν_{me} the effective magnetic diffusivity, β the thermal expansion coefficient, k_f the thermal conductivity of the fluid and k_s the thermal conductivity of the solid. The time derivative term is taken into consideration in Eq. (2) in order to allow the possibility of oscillatory convection.

The basic state is assumed to be quiescent and given by

$$\vec{q} = 0, \ P = P_b(z), \ \vec{B} = \vec{B}_b = B_0\hat{k}, \ T_{fb}(z) = T_{sb}(z) = -\frac{\Delta T}{d}z + T_l \quad (8)$$

where $\Delta T = T_l - T_u$. We superimpose infinitesimal disturbances on the basic state as follows:

$$\vec{q} = \vec{q}', \ P = P_b(z) + P', \ \vec{B} = B_o\hat{k} + \vec{B}', \ T_f = T_{fb}(z) + T_f', \ T_s = T_{sb}(z) + T_s' \quad (9)$$

where the prime indicates the perturbed quantity. For simplicity, we restrict our attention to two-dimensional magnetoconvection in a porous medium in the (x, z) plane and introduce the stream function for velocity and magnetic field in the form

$$\vec{q}' = \left(\frac{\partial \psi}{\partial z}, 0, -\frac{\partial \psi}{\partial x}\right), \quad \vec{B}' = \left(\frac{\partial \chi}{\partial z}, 0, -\frac{\partial \chi}{\partial x}\right). \quad (10a, b)$$

Substituting Eq. (9) into Eqs. (1)–(7), eliminating the pressure term from the momentum equation by operating curl once and non-dimensionalizing the variables by scaling x, y and z by d, t by d^2/κ_f, ψ by $\varepsilon\kappa_f$, χ by $B_0 d$, T_f' and T_s' by ΔT , where $\kappa_f = k_f/(\rho_0 c_p)_f$ is the effective thermal diffusivity of the fluid, we obtain the following dimensionless equations (after dropping the primes):

$$\left[\frac{1}{Pr}\frac{\partial}{\partial t} - \nabla^2 + Da^{-1}\right]\nabla^2\psi = -R\frac{\partial T_f}{\partial x} + Q\tau \frac{\partial}{\partial z}(\nabla^2\chi) - Q\tau J(\chi, \nabla^2\chi) + \frac{1}{Pr} J(\psi, \nabla^2\psi) \quad (11)$$

$$\frac{\partial \chi}{\partial t} = \frac{\partial \psi}{\partial z} + \tau \nabla^2 \chi + J(\psi, \chi) \quad (12)$$

$$\frac{\partial T_f}{\partial t} = -\frac{\partial \psi}{\partial x} + \nabla^2 T_f + H(T_s - T_f) + J(\psi, T_f) \tag{13}$$

$$\alpha \frac{\partial T_s}{\partial t} = \nabla^2 T_s - \gamma H(T_s - T_f). \tag{14}$$

Here, $R = \beta g \Delta T d^3/\nu\kappa_f$ is the Rayleigh number, $Q = B_0^2 d^2/\mu_m \rho_0 \nu \nu_{me}$ is the Chandrasekhar number, $\tau = \nu_{me}/\kappa_f$ is the ratio of magnetic to thermal diffusivity, $Pr = \nu/\kappa_f$ is the Prandtl number, $Da = K/d^2$ is the Darcy number, $H = hd^2/\varepsilon k_f$ is the inter-phase heat transfer coefficient, $\gamma = \varepsilon k_f/(1-\varepsilon) k_s$ is the porosity modified conductivity ratio and $\alpha = \kappa_f/\kappa_s$ is the ratio of thermal diffusivities. The nature of magnetoconvection depends crucially on the ratioτ. In laboratory experiments or in the Earth's core, τ is large (Cowling [34]) and in the astrophysical context it is usually very small owing to radiative heat transport.

The isothermal boundaries are considered to be stress-free. The appropriate boundary conditions are:

$$\psi = \frac{\partial^2 \psi}{\partial z^2} = \frac{\partial \chi}{\partial z} = T_f = T_s = 0 \text{ at } z = 0, 1. \tag{15}$$

3 Linear stability analysis

We neglect the nonlinear terms from Eqs. (11)–(14) and introduce the normal mode solutions of the form

$$\begin{aligned} \psi = A_1 \cos(ax)\sin(\pi z)\exp(\sigma t), \quad \chi = A_2 \cos(ax)\cos(\pi z)\exp(\sigma t) \\ (T_f, T_s) = (A_3, A_4)\sin(ax)\sin(\pi z)\exp(\sigma t) \end{aligned} \tag{16}$$

where a is the horizontal wave number, σ is the growth rate and A_1 to A_4 are constants. Substituting Eq. (16) into the linearized version of Eqs. (11)–(14) and eliminating the constants A_1 to A_4, we obtain an expression for the Rayleigh number in the form

$$R = \frac{\left[(\frac{\sigma}{Pr} + \delta^2 + Da^{-1})(\sigma + \tau\delta^2)\delta^2 + Q\tau\pi^2\delta^2\right]}{a^2(\sigma + \tau\delta^2)} \left\{(\sigma + \delta^2 + H) - \frac{\gamma H^2}{(\alpha\sigma + \delta^2 + \gamma H)}\right\} \tag{17}$$

where $\delta^2 = \pi^2 + a^2$. Now we set the real part of σ equal to zero and let $\sigma = i\omega$ in the above equation to examine the stability of the system. After clearing the complex quantities from the denominator, Eq. (17) yields

$$R = \frac{\delta^2}{a^2 Pr(\tau^2\delta^4 + \omega^2)\left\{(\delta^2 + \gamma H)^2 + \alpha^2\omega^2\right\}}(\Delta_1 + i\omega\,\Delta_2) \tag{18}$$

where

$$\begin{aligned} \Delta_1 = {} & \delta^2(\delta^4 + \alpha^2\omega^2)\left\{\pi^2 Pr Q\tau(\tau\delta^4 + \omega^2) + (Da^{-1}Pr\delta^2 + Pr\delta^4 - \omega^2)(\tau\delta^4 + \omega^2)\right\} \\ & + \delta^2 H^2\gamma(\tau\delta^4 + \omega^2)\left\{Da^{-1}Pr(1+\gamma)\delta^2 + Pr(1+\gamma)\delta^4 - (\alpha+\gamma)\omega^2\right\} \\ & + \delta^2 H^2\gamma\pi^2 Pr Q\tau\left\{\tau(1+\gamma)\delta^4 + (\alpha+\gamma)\omega^2\right\} \\ & + \delta^4 H\gamma\pi^2 Pr Q\tau\left\{2\gamma\omega^2 + \tau(1+2\gamma)\delta^4 + \alpha^2\omega^2\right\} \\ & + \delta^2 H(\tau\delta^4 + \omega^2)\left\{Da^{-1}Pr(1+2\gamma)\delta^4 + Da^{-1}Pr\alpha^2\omega^2 - 2\delta^2\gamma\omega^2\right\} \\ & + \delta^2 H(\tau\delta^4 + \omega^2)Pr\delta^2(\delta^4 + 2\gamma\delta^4 + \alpha^2\omega^2) \end{aligned} \tag{19}$$

$$\begin{aligned}\Delta_2 = {} & \delta^2(\delta^4+\alpha^2\omega^2)\left\{\pi^2 Pr Q(\tau-1)\tau\delta^2 + (Da^{-1}Pr + (1+Pr)\delta^2)(\tau\delta^4+\omega^2)\right\} \\ & + \delta^4 H^2\gamma\pi^2 Pr Q\tau\left\{(\alpha+\gamma)\tau - 1 - \gamma\right\} + \delta^2 H\pi^2 Pr Q\tau\left\{2(\tau-1)\delta^4\gamma - \delta^4 - \alpha^2\omega^2\right\} \\ & + \delta^2 H^2\gamma\left\{Da^{-1}Pr(\alpha+\gamma) + (1+\gamma+Pr(\alpha+\gamma))\delta^2\right\}(\tau\delta^4+\omega^2) \\ & + \delta^2 H(\tau\delta^4+\omega^2)\left\{2Da^{-1}Pr\gamma\delta^2 + (1+2(1+Pr)\gamma)\delta^4 + \alpha^2\omega^2\right\}. \end{aligned} \tag{20}$$

Since R is a physical quantity, it must be real and from Eq. (18) it implies either $\omega = 0$ or $\Delta_2 = 0$. Accordingly, we obtain the condition for the occurrence of stationary or oscillatory convection.

3.1 Stationary convection

The stationary convection (direct bifurcation) corresponds to $\omega = 0$ and it occurs at

$$R^s = \frac{\delta^2\left[\delta^4 + a^2 Da^{-1} + (Da^{-1}+Q)\pi^2\right]}{a^2}\frac{\left[\delta^2 + H(1+\gamma)\right]}{(\delta^2+\gamma H)}. \tag{21}$$

When $Q = 0$, Eq. (21) reduces to

$$R^s = \frac{\delta^4\left[\delta^2 + Da^{-1}\right]}{a^2}\frac{\left[\delta^2 + H(1+\gamma)\right]}{(\delta^2+\gamma H)} \tag{22}$$

and coincides with Malashetty et al. [29]. If we set $Da^{-1} = 0$ and $H = 0$ in Eq. (21), we obtain

$$R^s = \frac{\delta^2(\delta^4 + Q\pi^2)}{a^2} \tag{23}$$

which coincides with Chandrasekhar [2]. The critical value of R^s with respect to wave number is computed numerically.

3.2 Asymptotic analysis

For small values of H, it is noted that there is almost no transfer of heat between the fluid and solid phases. The solid phase ceases to affect the thermal field of the fluid, which is free to act independently. On the other hand, for large H, the solid and fluid phases will have nearly identical temperatures and may be treated as a single phase.

Case 1: $H << 1$

For this case, the Rayleigh number R^s is slightly above the corresponding value for the LTE case. Accordingly, we expand R^s given by Eq. (21) in a power series in H as

$$R^s = \frac{\delta^2\left[\delta^4 + a^2 Da^{-1} + (Da^{-1}+Q)\pi^2\right]}{a^2}\left[1 + \frac{H}{\delta^2} - \frac{\gamma H^2}{\delta^4} + \cdots\right]. \tag{24}$$

To minimize R^s up to $O(H^2)$, we set $\partial R^s/\partial a = 0$ and obtain an expression of the form

$$\begin{aligned} & 2(a^2+\pi^2)^2\left\{2a^6 + a^4(Da^{-1}+3\pi^2) - \pi^4(Da^{-1}+Q+\pi^2)\right\} \\ & + 2H(a^2+\pi^2)^2\left\{a^4 - \pi^2(Da^{-1}+Q+\pi^2)\right\} \\ & + 2H^2\gamma\left\{a^4(Da^{-1}+\pi^2) + 2a^2\pi^2(Da^{-1}+Q+\pi^2) + \pi^4(Da^{-1}+Q+\pi^2)\right\} \\ & + \cdots = 0. \end{aligned} \tag{25}$$

We also expand a in power series of H as

$$a = a_0 + a_1 H + a_2 H^2 + \cdots \tag{26}$$

where a is the critical wave number for the LTE case. Substituting Eq. (26) into Eq. (24) and equating the coefficients of the same powers of, H we find a_1 and a_2, and they are given by

$$a_1 = \frac{\Delta_3}{\Delta}, \quad a_2 = \frac{\Delta_4}{\Delta} \tag{27}$$

where,

$$\begin{aligned}
\Delta_3 &= 2(a_0^2+\pi^2)^2\left\{a_0^4 - \pi^2(Da+\pi^2+Q)\right\}\\
\Delta_4 &= 2\{8a_0^7a_1 + 90a_0^8a_1^2 + 12a_0^5a_1\pi^2 + 28a_0^6a_1^2(Da+7\pi^2) - 4a_0^3a_1\pi^2(Da+Q)\\
&\quad - 4a_0a_1\pi^4(Da+Q+\pi^2) - \pi^4(Da+Q+\pi^2)(2a_1^2\pi^2-\gamma) + a_0^4 30a_1^2\pi^2(Da+4\pi^2)\\
&\quad + a_0^4(Da+\pi^2)\gamma + 2a_0^2\pi^2a_1^2(6\pi^4 - 3\pi^2Q)) + 2a_0^2\pi^2(Da+Q+\pi^2)\gamma\}\\
\Delta &= -8a_0(a_0^2+\pi^2)(5a_0^6 + a_0^2\pi^2(Da+3\pi^2) + a_0^4(2Da+9\pi^2) - \pi^4(Da+\pi^2+Q)).
\end{aligned} \tag{28}$$

With these values of a_0, a_1 and a_2, Eq. (26) gives the critical wave number and consequently using this in Eq. (24) one can obtain the critical Rayleigh number for small H.

Case 2: $H >> 1$

For this case, the Rayleigh number takes the form

$$\begin{aligned}
R^s = \frac{(1+\gamma)}{\gamma}\frac{\delta^2\left[\delta^4 + a^2Da^{-1} + (Da^{-1}+Q)\pi^2\right]}{a^2}\\
\times\left[1 - \frac{\delta^2}{\gamma\{\gamma+1\}}\frac{1}{H} + \frac{\delta^4}{\gamma^2\{\gamma+1\}}\frac{1}{H^2} + \cdots\right]
\end{aligned} \tag{29}$$

To minimize R^s up to $O(H^2)$, we set $\partial R^s/\partial a = 0$ and obtain an expression of the form

$$\begin{aligned}
&-2\gamma^2(1+\gamma)\left\{2a^6 + a^4(Da^{-1}+3\pi^2) - \pi^4(Da^{-1}+Q+\pi^2)\right\}\\
&+2H\gamma\left\{3a^8 + 2a^6(Da^{-1}+4\pi^2) - \pi^6(Da^{-1}+Q+\pi^2) + a^4\pi^2(3Da^{-1}+Q+6\pi^2)\right\}\\
&-2H^2(a^2+\pi^2)^2\left\{\begin{array}{l} 4a^6 + a^4(3Da^{-1}+7\pi^2)\\ +2a^2\pi^2(Da^{-1}+Q+\pi^2) - \pi^4(Da^{-1}+Q+\pi^2)\end{array}\right\} + \cdots = 0.
\end{aligned} \tag{30}$$

We also expand a in power series of H as

$$a = a_0 + \frac{a_1'}{H} + \frac{a_2'}{H^2} + \cdots \tag{31}$$

where a_0 is the critical wave number for the LTE case and a_1' and a_2' are to be determined. Substituting Eq. (31) into Eq. (29) and equating the coefficients of like powers of H we find a_1' and a_2'. They are given by

$$a_1' = \frac{\Delta_3'}{\Delta'}, \quad a_2' = \frac{\Delta_4'}{\Delta'} \tag{32}$$

where

$$\begin{aligned}
\Delta_3' &= -2\left\{(3a_0^8 + 2a_0^6(Da + 4\pi^2) - \pi^6(Da + \pi^2 + Q) + a_0^4\pi^2(3Da + 6\pi^2 + Q)\right\}\gamma \\
\Delta_4' &= -2\{-4a_0^{10} - 3a_0^8(Da + 5\pi^2) + \pi^8(Da + \pi^2 + Q) - 2a_0^6\pi^2(4Da + 10\pi^2 + Q) \\
&\quad + 24a_0^7a_1\gamma + 12a_0^5a_1(Da + 4\pi^2)\gamma + 4a_0^3a_1\pi^2(3Da + 6\pi^2 + Q)\gamma \\
&\quad - 6a_0^2a_1^2(Da + 3\pi^2)\gamma^2(1 + \gamma) - a_0^4(6Da\pi^4 + 10\pi^6 + 3\pi^4Q + 30a_1^2\gamma^2(1 + \gamma))\} \\
\Delta' &= -8a_0^3(3a_0^2 + Da + 3\pi^2)\gamma^2(1 + \gamma) \qquad (33)
\end{aligned}$$

Again with these values of a_0, a_1' and a_2', we compute the critical wave number a_c from Eq. (31) and finally using this value of a_c one can obtain the critical Rayleigh number R_c^s from Eq. (29) for large H. The expression for the critical Rayleigh number R_c^s and the critical wave number a_c for both small and large values of H are evaluated and compared with the exact values obtained from Eq. (21) in Table 1. We note that there is an excellent agreement between these two results.

3.3 Oscillatory convection

The oscillatory convection (Hopf bifurcation) corresponds to $\Delta_2 = 0\,(\omega \neq 0)$ in Eq. (18) and this condition gives a dispersion relation of the form

$$c_1(\omega^2)^2 + c_2(\omega^2) + c_3 = 0 \qquad (34)$$

where

$$\begin{aligned}
c_1 &= \delta^2\alpha^2\left\{H + Da^{-1}Pr + (1 + Pr)\gamma\right\} \\
c_2 &= \delta^2H^2\gamma\left\{Da^{-1}Pr(\alpha + \gamma) + (1 + \gamma + Pr(\alpha + \gamma))\delta^2\right\} \\
&\quad + \delta^2H\left\{2Da^{-1}Pr\gamma\delta^2 - \pi^2PrQ\tau\alpha^2\right\} + \delta^6H\left\{1 + \tau^2\alpha^2 + 2(1 + Pr)\gamma\right\} \\
&\quad + \delta^4\left\{\pi^2PrQ(\tau - 1)\tau\alpha^2 + (1 + \tau^2\alpha^2)\delta^2(Da^{-1}\,\mathrm{Pr} + \delta^2 + \delta^2Pr)\right\} \\
c_3 &= \tau\delta^4\left\{H^2\pi^2PrQ\gamma((\alpha + \gamma)\tau - 1 - \gamma) + H\pi^2PrQ(2(\tau - 1)\gamma - 1)\delta^2\right\} \\
&\quad + \tau\delta^4\left\{\pi^2PrQ(\tau - 1)\delta^4 + 2Da^{-1}HPr\,\tau\gamma\delta^4 + H\tau(1 + 2(1 + Pr)\gamma)\delta^6\right\} \\
&\quad + \tau^2\delta^{10}\left\{Da^{-1}Pr(1 + Pr)\delta^2\right\} + \tau^2\delta^6H^2\gamma\left\{Da^{-1}Pr(\alpha + \gamma)\right. \\
&\quad \left. + \delta^2(1 + \gamma + Pr(\alpha + \gamma))\right\}. \qquad (35)
\end{aligned}$$

When $\Delta_2 = 0\,(\omega \neq 0)$, Eq. (18) gives an expression for the oscillatory Rayleigh number and the oscillatory convection occurs at $R = R^o$, where

$$R^o = \frac{\delta^2\Delta_1}{a^2Pr(\tau^2\delta^4 + \omega^2)\left\{(\delta^2 + \gamma H)^2 + \alpha^2\omega^2\right\}}. \qquad (36)$$

The critical value of R^o with respect to the wave number is determined as follows. For fixed parametric values, Eq. (34) is solved first to determine the positive values of ω^2. If there are none, then no oscillatory convection is possible. If there is only one positive value of ω^2 then the critical value of R^o with respect to wave number is computed numerically from Eq. (36). If there are two positive values of ω^2, then the minimum of R^o amongst these two ω^2 is retained to find the critical value of R^o with respect to the wave number.

Table 1 Comparison of asymptotic (A) and exact (E) values of the critical Rayleigh number (R_c) and the critical wave number (a_c) for different values of H with $Da^{-1} = 100$ and $\gamma = 1$

Q	$\log_{10} H$	$R_c(A)$	$a_c(A)$	$R_c(E)$	$a_c(E)$
0	−2.0	4701.69	2.923	4701.69	2.923
	−1.0	4724.49	2.929	4724.5	2.929
	0.0	4935	2.978	4939.18	2.978
	1.0	5922.7	2.582	6316.63	1.448
	2.0	8685.71	3.012	8685.82	3.014
	3.0	9313.2	2.933	9313.18	2.933
	4.0	9389.63	2.924	9389.63	2.924
	5.0	9397.41	2.923	9397.41	2.923
	6.0	93,918	2.923	93,918	2.923
	7.0	93,918	2.923	93,926	2.923
100	−2.0	6656.56	3.402	6656.56	3.402
	−1.0	6684.32	3.409	6684.32	3.409
	0.0	6686.44	3.466	6947.05	3.466
	1.0	6742.14	3.124	8706.91	3.686
	2.0	12,172.6	3.538	12,111.5	3.538
	3.0	13,167.0	3.418	13,166.9	3.418
	4.0	13,292.7	3.403	13,292.7	3.403
	5.0	13,305.5	3.401	13,305.5	3.401
	6.0	13,306.8	3.401	13,306.8	3.401
	7.0	13,306.9	3.401	13,306.9	3.401
1000	−2.0	20,330.0	4.959	20,330.0	4.959
	−1.0	20,382.8	4.969	20,382.8	4.969
	0.0	20,889.2	5.053	20,889.7	5.054
	1.0	24,526.8	4.937	24,644.0	5.472
	2.0	36,090.6	5.423	35,195	5.407
	3.0	39,966.3	5.019	39,965.4	5.019
	4.0	40,573	4.965	40,573	4.965
	5.0	40,641.1	4.959	40,641.1	4.959
	6.0	40,647.4	4.959	40,647.4	4.959
	7.0	40,641	4.959	40,641	4.959

4 Weakly nonlinear stability analysis

The linear stability analysis discussed in the previous section provides only boundaries for instability due to its inherent nature. In this section, we consider a weakly nonlinear stability analysis using a truncated representation of Fourier series and construct model equations consisting of nonlinear autonomous ordinary differential equations. The very truncated Fourier series might not represent correctly the detailed dynamics within boundary layers that may form at high Rayleigh number values. Nevertheless, the model is expected to represent qualitatively well the effects related to the overall dynamics of the system with minimum amount of mathematical analysis and is a step forward towards understanding the full nonlinear problem. A minimal double Fourier series that describes the weakly nonlinear free convection is given by

$$\psi = \frac{2\sqrt{2}}{a}\delta A(t)\sin(ax)\sin(\pi z)$$
$$T_f = \frac{2\sqrt{2}}{\delta}B(t)\cos(ax)\sin(\pi z) - \frac{C(t)}{\pi}\sin(2\pi z)$$
$$T_s = \frac{2\sqrt{2}}{\delta}D(t)\cos(ax)\sin(\pi z) - \frac{E(t)}{\pi}\sin(2\pi z)$$
$$\chi = \frac{2\sqrt{2}}{\delta a}\pi F(t)\sin(ax)\cos(\pi z) - \frac{G(t)}{a}\sin(2ax) \tag{37a-d}$$

where the amplitudes A, B, C, D, E, F and G are functions of time and are to be determined from the dynamics of the system. Substituting Eq. (37a–d) into Eqs. (11)–(14) and equating the coefficients of like terms, we obtain the following nonlinear autonomous system of ordinary differential equations:

$$\frac{dA}{dt} = -Pr\delta^2\left[(1+\frac{Da^{-1}}{\delta^2})A + \frac{a^2}{\delta^6}R\,B + \frac{Q\tau}{\delta^4}\pi^2 F - \frac{Q\tau}{\delta^4}\pi^2(\varpi-3)\,FG\right]$$
$$\frac{dB}{dt} = -\delta^2 A - (\delta^2+H)B + \delta^2 AC + HD$$
$$\frac{dC}{dt} = -\delta^2\left[(\varpi+\frac{H}{\delta^2})C - \varpi AB - \frac{H}{\delta^2}E\right]$$
$$\frac{dD}{dt} = -\frac{1}{\alpha}\left[(\delta^2+\gamma H)D - \gamma HB\right]$$
$$\frac{dE}{dt} = -\frac{\delta^2}{\alpha}\left[(\varpi+\frac{\gamma H}{\delta^2})E - \frac{\gamma H}{\delta^2}C\right]$$
$$\frac{dF}{dt} = \delta^2\left[A - \tau F - AG\right]$$
$$\frac{dG}{dt} = \delta^2\left[\varpi AF - (4-\varpi)\tau G\right] \tag{38a-g}$$

where $\varpi = 4\pi^2/\delta^2$. Equation (38a–g) are the basic set that will be studied here. These equations possess two significant properties. First, the divergence of the flow in phase space

$$\frac{\partial\dot{A}}{\partial A} + \frac{\partial\dot{B}}{\partial B} + \frac{\partial\dot{C}}{\partial C} + \frac{\partial\dot{D}}{\partial D} + \frac{\partial\dot{E}}{\partial E} + \frac{\partial\dot{F}}{\partial F} + \frac{\partial\dot{A}G}{\partial G}$$
$$= \left[pr(\delta^2+Da^{-1}) + (\delta^2+H) + (4\pi^2+H) + \frac{(\delta^2+\gamma H)}{\alpha}\right.$$
$$\left. + \frac{(4\pi^2+\gamma H)}{\alpha} + (\pi^2+5a^2)\tau\right] \tag{39}$$

is always negative and so the solutions are attracted to a set of measure zero in the phase space: this may be a fixed point, a limit cycle or a strange attractor. The dot above a quantity denotes the derivative with respect to time. Second, the equations have an important symmetry as they are unchanged under the transformation

$$(A, B, C, D, E, F, G) \to (-A, -B, C, -D, E, -F, G). \tag{40}$$

The nonlinear system of autonomous differential equations (38a–g) is not amenable to analytical treatment, in general. Nonetheless, for the steady case the solution can be obtained at once. Such solutions are useful because they predict that a finite amplitude solution to the

system is possible for subcritical values of the Rayleigh number or not and that the minimum values of R for which a steady solution is possible lies below the critical values of R^s or R^o. Setting the left-hand sides of Eq. (38a–g) equal to zero, we obtain

$$\begin{aligned}
&\left(1+\frac{Da^{-1}}{\delta^2}\right)A+\frac{a^2}{\delta^6}\,R\,B+\frac{Q\tau}{\delta^4}\pi^2F-\frac{Q\tau}{\delta^4}\pi^2(\varpi-3)\,FG=0\\
&-\delta^2A-(\delta^2+H)B+\delta^2AC+HD=0\\
&\left(\varpi+\frac{H}{\delta^2}\right)C+\varpi AB-\frac{H}{\delta^2}E=0\\
&\left(\delta^2+\gamma H\right)D-\gamma HB=0\\
&\left(\varpi+\frac{\gamma H}{\delta^2}\right)E-\frac{\gamma H}{\delta^2}C=0\\
&A-\tau F-AG=0\\
&\varpi AF-\tau(4-\varpi)G=0.
\end{aligned}\tag{41a-g}$$

Expressing the amplitudes B, C, D, E, F and G in terms of A using Eq. (41a–g), we obtain

$$\begin{aligned}
&B=-\frac{L_3A}{L_1+L_2A^2},\quad C=\frac{L_2A^2}{L_1+L_2A^2},\quad D=-\frac{\gamma H(4\pi^2+\gamma H+H)A}{L_1+L_2A^2}\\
&E=\frac{\gamma H(\delta^2+\gamma H)A^2}{L_1+L_2A^2},\quad F=\frac{A\varsigma}{\tau(A^2+\zeta)},\quad G=\frac{A^2}{A^2+\zeta},
\end{aligned}\tag{42a-f}$$

where

$$\begin{aligned}
&\zeta=\frac{\tau^2(4-\varpi)}{\varpi}L_1=(\delta^2+\gamma H+H),(4\pi^2+\gamma H+H)L_2=(\delta^2+\gamma H)(4\pi^2+\gamma H)\\
&L_3=(\delta^2+\gamma H)(4\pi^2+\gamma H+H).
\end{aligned}\tag{43}$$

Substituting for B, C, D, E, F and G from Eq. (42a–f) in Eq. (41a), we obtain an expression for the finite amplitude Rayleigh number in the form

$$R^f=\frac{\delta^6}{a^2}\left[\frac{L_1+L_2A^2}{L_3}\right]\left\{\left(1+\frac{Da^{-1}}{\delta^2}\right)+\frac{Q\pi^2\zeta\left\{\zeta+(4-\varpi)A^2\right\}}{\delta^4(A^2+\zeta)^2}\right\}.\tag{44}$$

From the above equation, we get back the linear stability theory results for the steady case when $A=0$. When $Da^{-1}=0=H$, Eq. (44) reduces to the expression obtained by Knobloch et al. [7]. The minimum value of R^f obtained with respect to A^2 is termed as $R^f_{\min}$.

To investigate the behavior of steady finite amplitude solution in the neighborhood of R^s, we use perturbation theory. Accordingly, R is expanded in terms of the amplitude $A^2(A<<1)$ in the form

$$R=R^s+R_2A^2+O(A^4).\tag{45}$$

Equation (44) can be expanded in terms of A^2 to get

$$d_0(A^2)^3+d_1(A^2)^2+d_2(A^2)+d_3=0\tag{46}$$

where

$$
\begin{aligned}
d_0 &= \pi^4\delta^4 L_2(Da^{-1}+\delta^2)\\
d_1 &= \pi^2\left\{\delta^4(L_1\pi^2+2L_2\tau^2a^2)(Da^{-1}+\delta^2)-a^2L_3\pi^2R+4L_2\tau^2a^4\pi^2Q\right\}\\
d_2 &= -\tau^2a^2\left\{(2L_3R-4L_1Q-L_2\tau^2\delta^2Q)a^2\pi^2-\delta^4(L_2\tau^2\delta^2a^2+2L_1\pi^2)(Da^{-1}+\delta^2)\right\}\\
d_3 &= \tau^4a^4\left\{L_1\pi^2Q\delta^2+L_1Da^{-1}\delta^4+L_1\delta^6-L_3a^2R\right\}.
\end{aligned}
\tag{47}
$$

Equation (45) is substituted into Eq. (46) and the coefficients of like powers of A^2 are collected. At zeroth order of A^2, the results of linear stability are retrieved and at the order of A^2 we find that

$$
R_2=\frac{L_2\,\tau^2\delta^2a^2(\delta^4+Da^{-1}\delta^2+Q\pi^2)+2L_1\,Q\pi^4(a^2-\pi^2)}{a^4L_3\,\tau^2}. \tag{48}
$$

When $Da^{-1}=H=0$, Eq. (48) reduces to

$$
R_2=\frac{\delta^2}{a^2}(\delta^4+Q\pi^2)+\frac{2Q\pi^4(a^2-\pi^2)}{a^4\tau^2} \tag{49}
$$

and this result coincides with Knobloch et al. [7]. The quantity R_2 may be either positive or negative. The finite amplitude solution in the neighborhood of R^s is said to be stable if $R_2>0$ (supercritical) and unstable if $R_2<0$ (subcritical). From Eq. (48) it is evident that R_2 is always positive for all $a\geq\pi$ (i.e., vertically elongated cells).

4.1 Heat transport

The vigor of convection is measured in terms of heat and mass transfer. If H_t is the rate of heat transport per unit area then

$$
H_t=-\kappa_f\left\langle\frac{\partial T_{f_{total}}}{\partial z}\right\rangle_{z=0} \tag{50}
$$

where the angular brackets correspond to a horizontal average and

$$
T_{f_{total}}=T_0+\Delta T\left(1-\frac{z}{d}\right)+T_f(x,z,t). \tag{51}
$$

Substituting Eq. (37b) into Eq. (51) and using the resultant expression in Eq. (51), we get

$$
H_t=\frac{\kappa_f\Delta T}{d}(1+2c). \tag{52}
$$

The Nusselt number Nu is defined as

$$
Nu=\frac{H_t}{\kappa_f\Delta T/d}=1+2c=1+2\frac{L_2A^2}{L_1+L_2A^2}. \tag{53}
$$

For small amplitude convection, A^2 can be obtained from Eq. (45) and is given by

$$
A^2=\frac{(R-R^s)}{R_2}. \tag{54}
$$

5 Results and discussion

The effect of local thermal non-equilibrium (LTNE) on both linear and weakly nonlinear magnetoconvection in a layer of Brinkman porous medium is investigated. Figures 2 and 3 show the neutral stability curves on the (R, a)-plane for various values of physical parameters. The solid and dashed curves represent the stationary and the oscillatory modes, respectively. From these figures it is observed that the neutral stability curves exhibit single distinct minimum with respect to the wave number for different values of physical parameters. Increasing the porosity modified conductivity ratio γ (Fig. 2a) and decreasing the inter-phase heat transfer coefficient H (Fig. 2b) is to decrease both stationary and oscillatory Rayleigh numbers

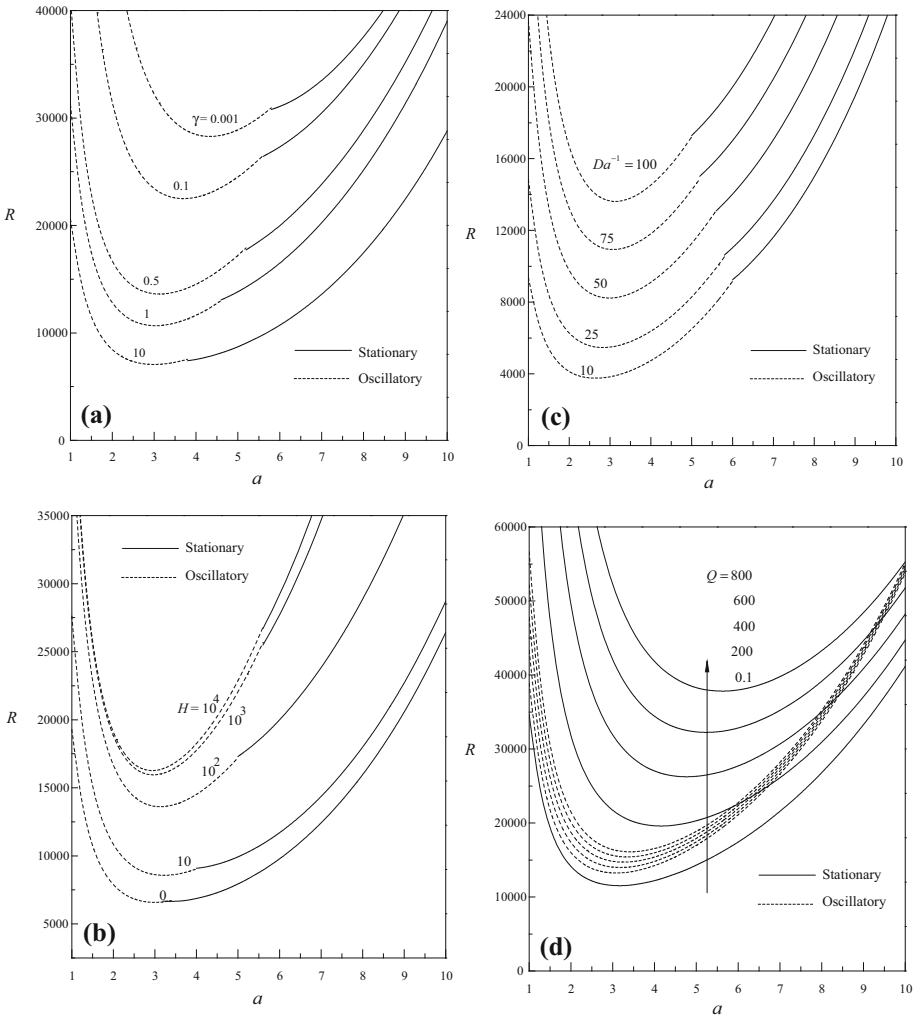

Fig. 2 Neutral curves for different values of **a** γ with $Q = 100 = Da^{-1}$, $\tau = 0.25$, $\alpha = 0.01$, $H = 100$, $Pr = 1$, **b** H with $Da^{-1} = 100 = Q$, $\tau = 0.25$, $\gamma = 0.5$, $Pr = 1$, $\alpha = 0.01$, **c** Da^{-1} with $Q = 100$, $\tau = 0.25$, $\alpha = 0.01$, $\gamma = 0.5$, $H = 100$, $Pr = 1$ and **d** Q with $Da^{-1} = 100$, $\tau = 0.25$, $\alpha = 0.01$, $\gamma = 0.5$, $H = 100$, $Pr = 1$

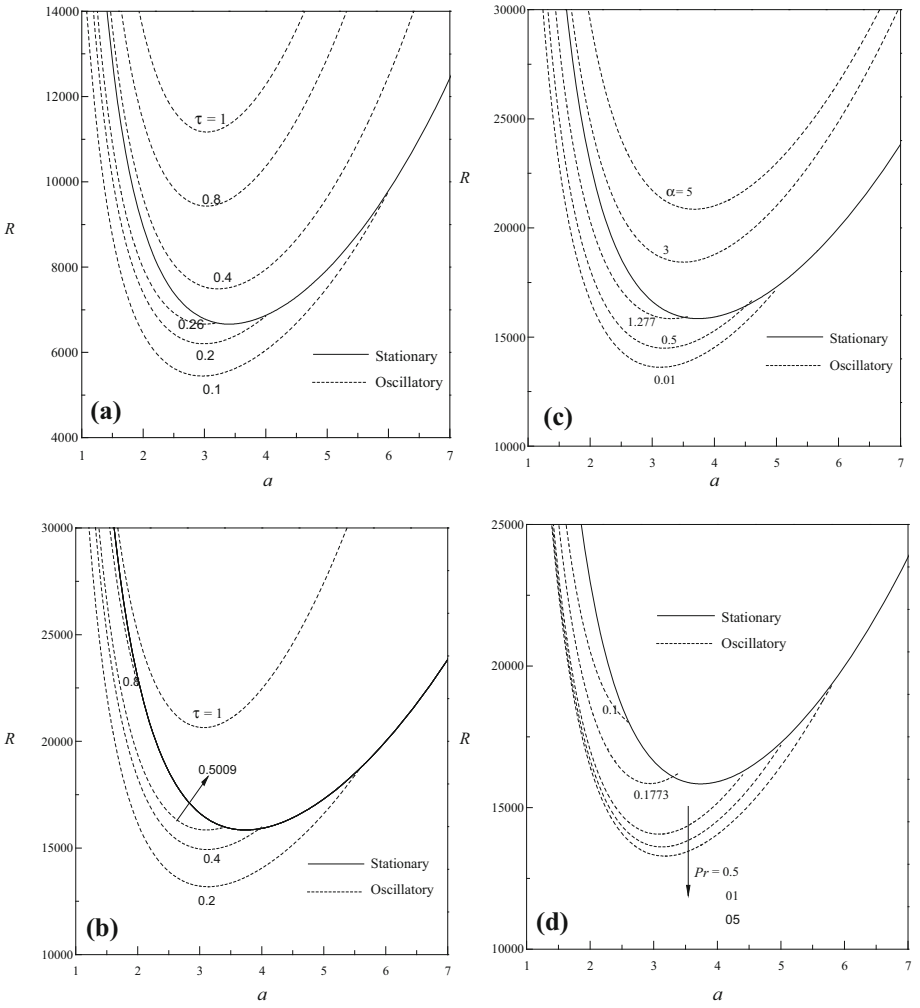

Fig. 3 Neutral curves for different values of **a** τ with $Da^{-1} = 100$, Q=100, $\alpha = 0.01$, $\gamma = 0.5$, $H = 0$ and $Pr = 1$, **b** τ with $Da^{-1} = 100$, Q=100, $\alpha = 0.01$, $\gamma = 0.5$, $H = 100$ and $Pr = 1$, **c** α with $Da^{-1} = 100$, Q=100, $\tau = 0.25$, $\gamma = 0.5$, $H = 100$ and $Pr = 1$, **d** Pr with $Da^{-1} = 100$, Q=100, $\tau = 0.25$, $\gamma = 0.5$, $H = 100$ and $\alpha = 0.01$

and also their effect is to shift the bifurcation wave number (i.e. the wave number at which the preferred mode of instability bifurcates) to the lower wave number region. The trend observed is quite opposite in nature with increasing inverse Darcy number Da^{-1} and the Chandrasekhar number Q and the same is evident from Fig. 2c, d, respectively.

The effect of ratio of magnetic diffusivity to thermal diffusivity τ alters only the oscillatory convection and its effect is to delay the oscillatory onset (Fig. 3a, b). Moreover, oscillatory convection is preferred over stationary convection provided the value of τ is less than unity as observed in the classical non-porous domain case (Chandrasekhar [2]). For the LTE case ($Da^{-1} = 100 = Q$, $Pr = 1$ and $H = 0$), oscillatory convection becomes a preferred mode of instability if $\tau < 0.26$ (Fig. 3a). The Rayleigh number for both steady and oscillatory onset coincides at $\tau = \tau^* = 0.26$ which corresponds to a co-dimension 2 point. For the LTNE case

Table 2 Values of τ^* at which steady and oscillatory Rayleigh numbers coincide for different values of Da^{-1} and H for $\gamma = 0.5,\ \alpha = 0.01,\ Pr = 1$ and $Q = 1000$

H	Da^{-1}	R^s	a_c	R^o	a_c	τ^*
0	10	30,519	3.645	30,519	2.841	0.493
	20	3460.98	3.598	3460.98	2.880	0.448
	50	4662.66	3.498	4662.66	2.945	0.352
	100	6653.46	3.401	6653.46	2.996	0.260
100	10	7175.78	3.957	7175.78	2.703	0.905
	20	8141.92	3.917	8141.92	2.790	0.827
	50	11,030.5	3.826	11,030.5	2.956	0.663
	100	15,826.1	3.734	15,826.1	3.099	0.502

with $\alpha = 0.01$, $\gamma = 0.5$, $Da^{-1} = 100 = Q$, $Pr = 1$ and $H = 100$ the value of τ^* is found to be 0.5009 (Fig. 3b). Thus the effect of LTNE is to increase the range of τ^* up to which the oscillatory convection is preferred over the stationary convection. The values of τ^* obtained for different values of Da^{-1} and H for $\gamma = 0.5, \alpha = 0.01,\ Pr = 1$ and $Q = 1000$ are tabulated in Table 2. From the table it is seen that increasing Da^{-1} is to decrease the value of τ^*. In addition, the value of τ^* for the LTE case is found to be lower than those of LTNE case for any fixed value of Da^{-1}. Similarly, the ratio of fluid to solid thermal diffusivities, α and the Prandtl number, Pr influences only the oscillatory convection. Increasing α is to increase the oscillatory Rayleigh number (Fig. 3c) while opposite is the case with increasing Pr (Fig. 3d). From these two figures also it is evident that the oscillatory convection is preferred only up to certain values of α and Pr. For the parametric values chosen, the value of α and Pr up to which the oscillatory convection is preferred is 1.277 and 0.1773, respectively and beyond which steady convection is found to be the preferred mode of instability.

The variation of critical Rayleigh and wave numbers for both stationary and oscillatory convection is shown in Figs. 4, 5, 6, 7, 8, 9 and 10 as a function of $\log_{10} H$ for various values of physical parameters. The comparison of results in these figures demonstrates the impact of various physical parameters on the preferred of mode (stationary or oscillatory) of instability. Figure 4a exhibits the variation of critical Rayleigh number R_c, computed with respect to wave number a, while Fig. 4b shows the variation of corresponding critical wave number a_c as a function of $\log_{10} H$ for different values of γ when $Q = 100$, $\tau = 0.25$, $\alpha = 0.01$, $Da^{-1} = 100$ and $Pr = 1$. It is seen that oscillatory convection is the preferred mode of instability for all values of γ considered. For a fixed non-zero value of γ, R_c increases steadily with H; reaches a maximum and remains unchanged thereafter with further increase in H. However, for $\gamma = 0$, R_c increases sharply as H increases. From the figure, it is also observed that R_c is independent of γ for smaller values of H and it remains almost independent of H for $\gamma \geq 10$. This is because, for very small values of H and higher values of γ there is no significant transfer of heat between the fluid and solid phases, and hence the condition for the onset of convection is not affected by the properties of the solid phase. This corresponds to classical LTE results. For other values of γ, however, R_c varies with γ as the value of H goes on increasing and remains independent of H at higher values of H. This may be attributed to the fact that at higher values of H, the condition for the onset of convection is based on the mean properties of the medium and hence the critical Rayleigh number varies with γ. The figures also indicate that for moderate and large values of H, the critical Rayleigh number decreases with the increasing values of γ. This is because, increase in the value of γ leads to significant transfer of heat through both by solid and fluid phases which in turn reduces the stabilizing effect of inter-phase heat transfer coefficient and hastens the onset of convection.

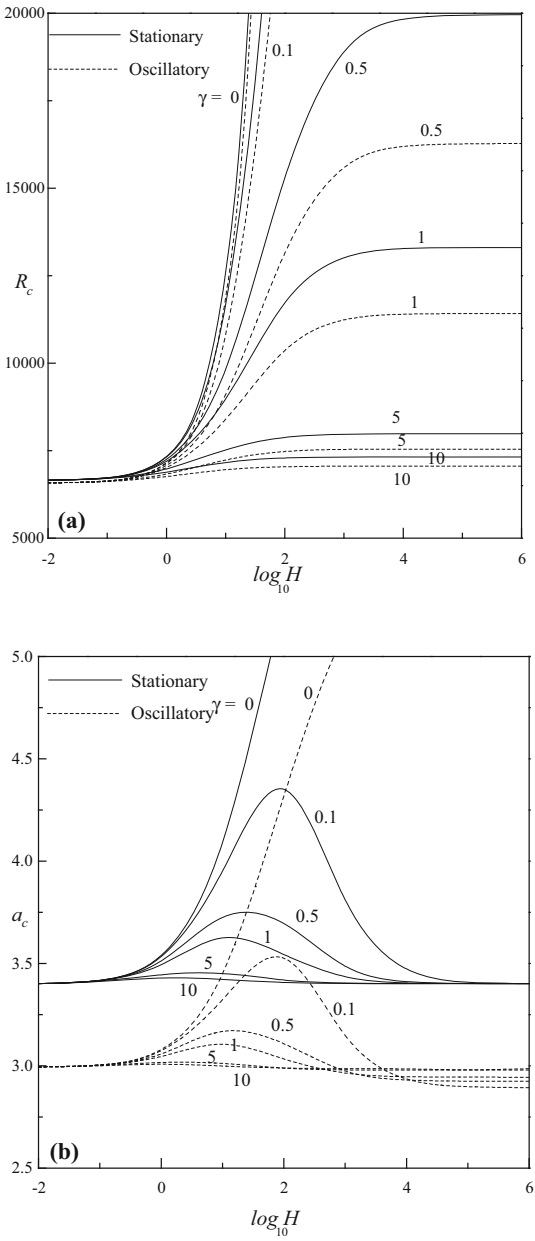

Fig. 4 Variation of **a** R_c and **b** a_c with $log_{10} H$ for different values of γ with $Q = 100$, $\tau = 0.25, \alpha = 0.01$, $Da^{-1} = 100$ and $Pr = 1$

Figure 4b indicates that a_c remains unaffected in the small-H as well as large-H limits, while at intermediate values of H (LTNE model) it attains a maximum value for different non-zero values of γ. Moreover, the critical wave number in the small and large-H limits is the same for all values of γ except when $\gamma = 0$, and in that case a_c rises sharply and appears to go to a vertical asymptote in the steady case. In the oscillatory case, however, the critical wave number differs for different values of γ in the large-H limit and their effect also gets reversed.

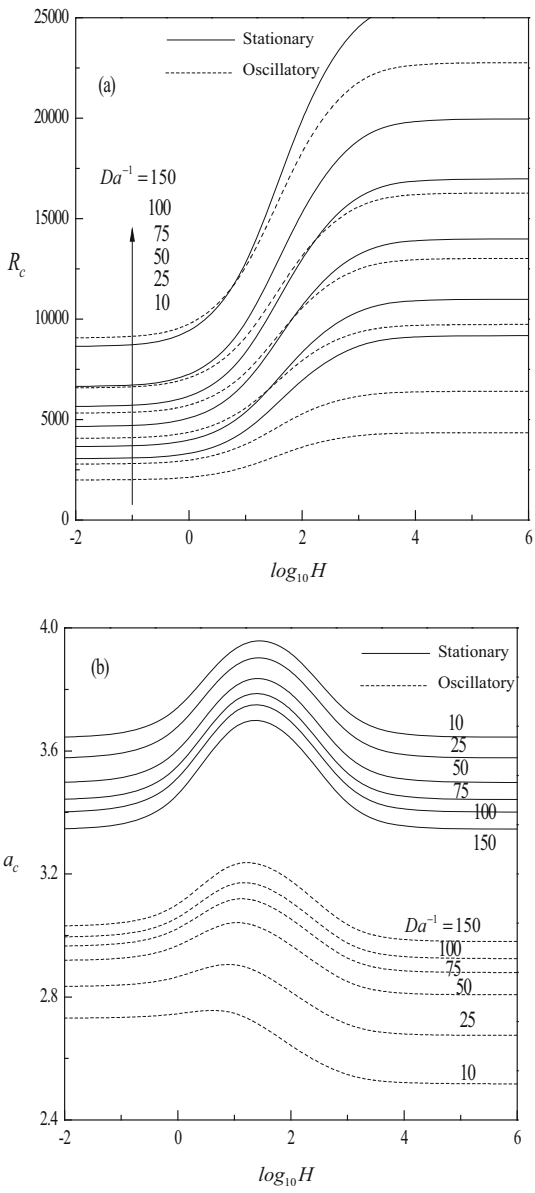

Fig. 5 Variation of **a** R_c and **b** a_c with $log_{10}H$ for different values of Da^{-1} with $Q = 100$, $\tau = 0.25$, $\alpha = 0.01$, $\gamma = 0.5$ and $Pr = 1$

At intermediate values of H, it is noted that an increase in the value of γ is to decrease the critical wave number and hence its effect is to increase the size of convection cells.

In Fig. 5a, b, the influence of inverse Darcy number Da^{-1} on R_c and a_c is displayed, respectively as a function of $\log_{10} H$ for $\gamma = 0.5$, $Q = 100$, $\tau = 0.25$, $\alpha = 0.01$, and $Pr = 1$. It is seen that increasing Da^{-1} is to delay the onset of both stationary and oscillatory convection. This is due to the fact that Da^{-1} is inversely related to the permeability of the porous medium. Therefore, increase in the value of Da^{-1} amounts to decrease in the permeability of the porous medium which retards the fluid flow. Therefore, higher heating is

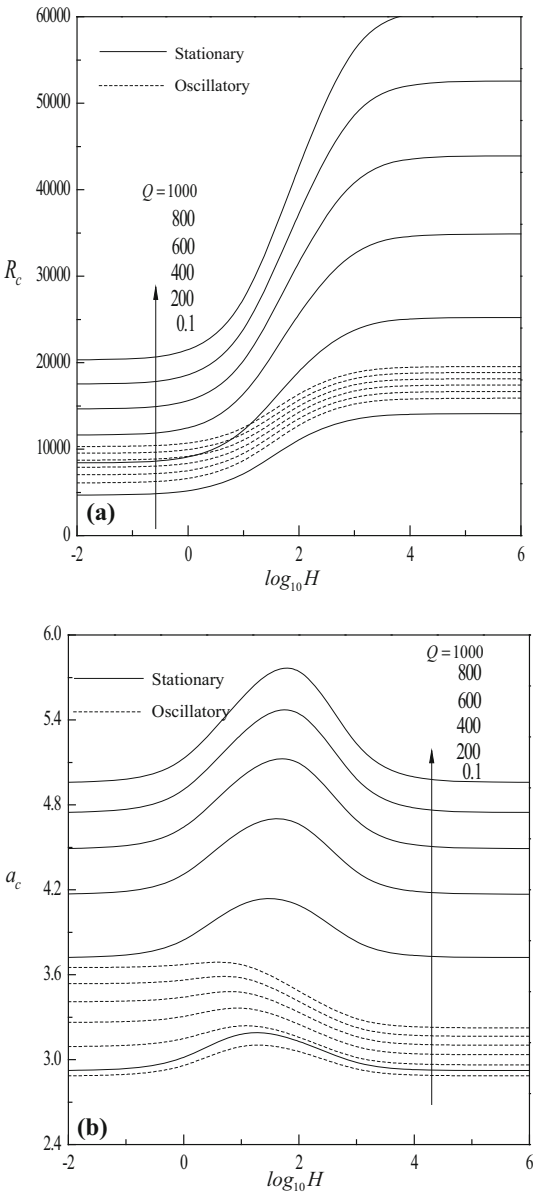

Fig. 6 Variation of **a** R_c and **b** a_c with $log_{10}H$ for different values of Q with $Da^{-1} = 100$, $\tau = 0.25, \alpha = 0.01, \gamma = 0.5$ and $Pr = 1$

required for the onset of convection. Although oscillatory convection is preferred to stationary convection for all values of Da^{-1}considered, a mixed behavior could be seen initially when $Da^{-1} = 150$. In this case, it is observed that stationary convection is preferred up to certain values of $\log_{10} H$ (Fig. 5a). The critical wave number is found to increase with Da^{-1} in the case of oscillatory convection, while an opposite trend is noticed in the case of stationary convection (Fig. 5b). Besides, the critical wave number in the small and large-H limits coincide in the stationary case but it assumes different values in the oscillatory case.

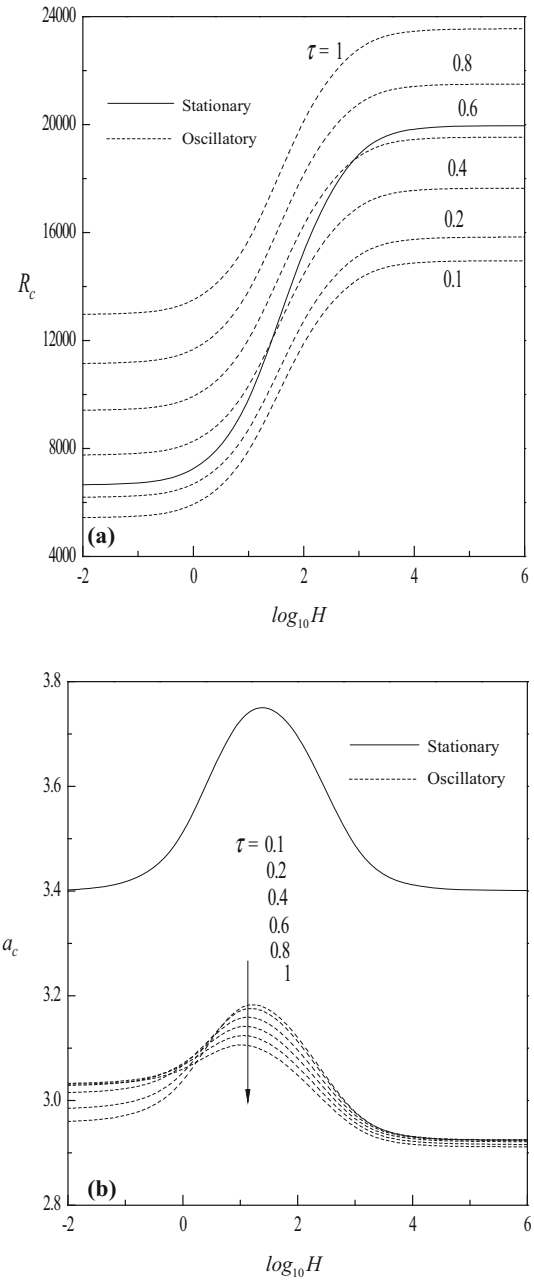

Fig. 7 Variation of **a** R_c and **b** a_c with $log_{10}H$ for different values of τ with $Da^{-1} = 100$, $Q = 100, \alpha = 0.01, \gamma = 0.5$ and $Pr = 1$

Figure 6a, b, respectively display the variation of R_c and a_c as a function of $\log_{10} H$ for various values of Chandrasekhar number Q when $Da^{-1} = 100, \tau = 0.25, \alpha = 0.01, \gamma = 0.5$ and $Pr = 1$. From the figures it is noted that increasing Q is to delay the onset of convection and also to decrease the size of convection cells. This is due to the fact that increasing Q leads to increase in the magnetic field strength and its effect is to suppress vertical motion and

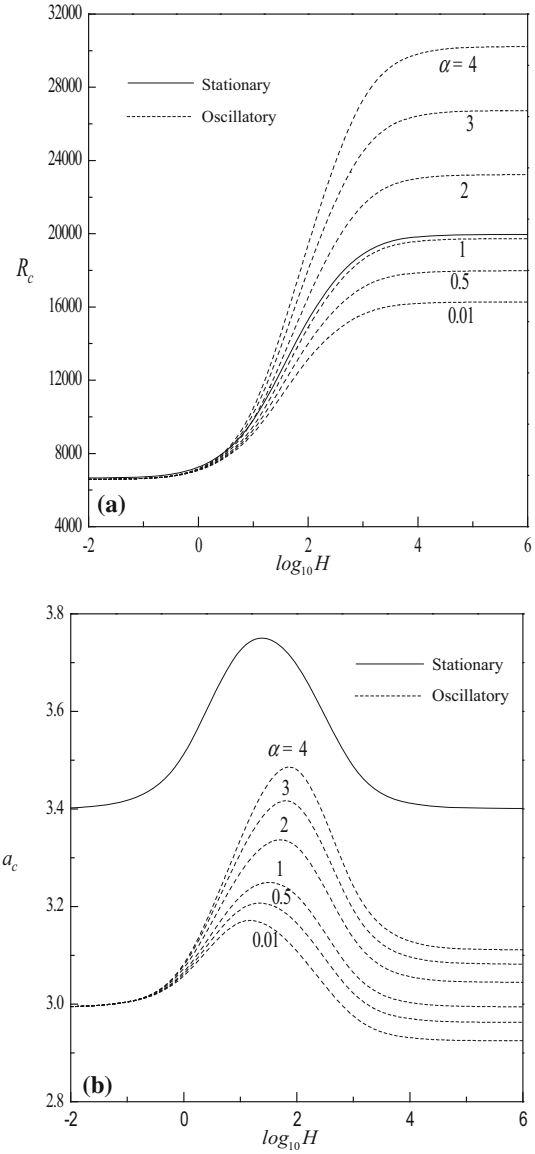

Fig. 8 Variation of **a** R_c and **b** a_c with $log_{10}H$ for different values of α with $Da^{-1} = 100$, $Q = 100$, $\tau = 0.25$, $\gamma = 0.5$ and $Pr = 1$

thereby restricts the motion to the horizontal plane. It is also seen the oscillatory convection is the preferred mode of instability for all values of Q except when $Q = 0.1$. In other words, oscillatory convection is preferred only when Q exceeds certain threshold value which in turn depends on the values of other physical parameters. The variation in the critical wave number with Q in the stationary case is found to be dominant when compared to oscillatory case. Here also it is observed that the critical wave number for small and large-H limits turns out to be same in the stationary case but it assumes different values in the oscillatory case.

The influence of ratio of magnetic to thermal diffusivities τ on critical Rayleigh number and wave number is illustrated in Fig. 7a, b, respectively as a function of $\log_{10} H$ for $Da^{-1} =$

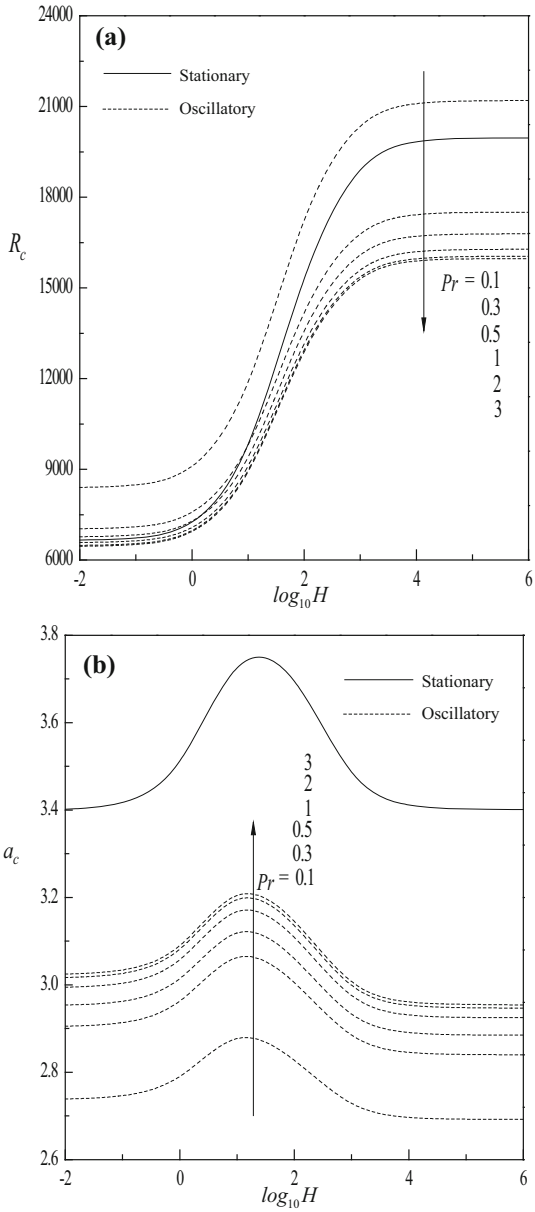

Fig. 9 Variation of **a** R_c and **b** a_c with $log_{10}H$ for different values of Pr with $Da^{-1} = 100$, $Q = 100$, $\tau = 0.25$, $\gamma = 0.5$ and $\alpha = 0.01$

100, $Q = 100$, $\alpha = 0.01$, $\gamma = 0.5$ and $Pr = 1$. It is observed that the effect of increasingτ is to delay the onset of oscillatory convection and it will be a preferred mode of instability only up to certain values τ depending on the value of H (Fig. 7a). The critical wave number decreases with increasing τ but not so significantly (Fig. 7b).

Figure 8a, b illustrate the effect of ratio of conductivities α on the stability characteristics of the system. The curves of R_c displayed as a function $\log_{10} H$ for $Da^{-1} = 100$, $Q = 100$, $\tau = 0.25$, $\gamma = 0.5$ and $Pr = 1$ in Fig. 8a reveal that increasing α is to delay the onset of

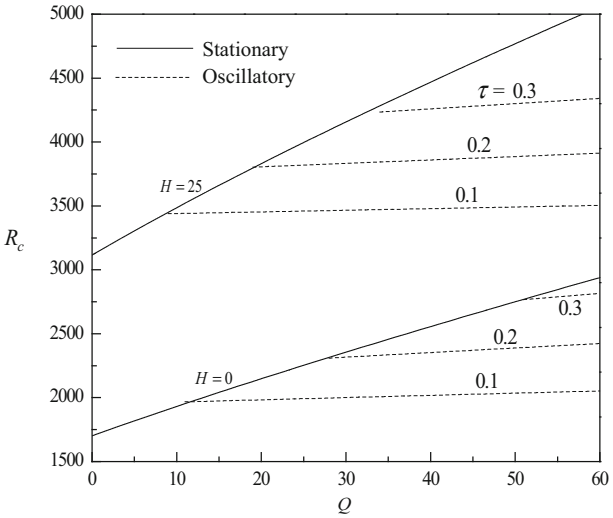

Fig. 10 Variation of critical Rayleigh number R_c with Q for different values of τ and H with $Da^{-1} = 25$, $\gamma = 0.5$, $\alpha = 0.01$ and $Pr = 1$

Table 3 Comparison of steady and finite amplitude Rayleigh numbers for different values of wave number a when $Da^{-1} = 0$, $H = 0$ and $Q = 1000 \times \pi^2$

a	Knobloch et al. [7]			Present analysis		
	R^s	$R^f_{\min}$		R^s	$R^f_{\min}$	
		$\tau = 0.4$	$\tau = 0.2$		$\tau = 0.4$	$\tau = 0.2$
$\pi/5$	2.54×10^6	10,607	6005	2.535×10^6	10,607.4	6004.8
$\pi/4$	1.66×10^6	11,263	5560	1.658×10^6	11,262.8	5560.2
$\pi/3$	9.76×10^5	13,937	5826	9.753×10^5	13,937.0	5826.3
$\pi/2$	4.88×10^5	23,107	8083	4.878×10^5	23,107.3	8082.7
$\pi/\sqrt{2}$	2.93×10^5	40,352	12,904	2.929×10^5	40,352.0	12,904.0
π	1.96×10^5	75,079	23,075	1.956×10^5	75,079.4	23,075.3

Table 4 Comparison of stationary and finite amplitude critical Rayleigh numbers for different values of H and τ for $\gamma = 0.5$, $Da^{-1} = 20$ and $Q = 1000$

H	R^s_c	a_c	$\tau = 0.2$			$\tau = 0.4$			$\tau = 1$		
			$(R^f_c)_{\min}$	a_c	A_c	$(R^f_c)_{\min}$	a_c	A_c	$(R^f_c)_{\min}$	a_c	A_c
0	16,287	5.495	2275.8	2.201	0.445	3007.3	2.028	0.557	3461.0	3.598	0
10	19,641	6.094	3093.0	2.462	0.552	3962.2	2.257	0.707	4651.5	3.944	0
20	22,209.9	6.356	3545	2.520	0.609	4451.7	2.318	0.789	6924.6	2.181	0.963
50	27,703.5	6.602	4216.0	2.534	0.963	5116.8	2.350	0.911	7641.1	2.090	1.197
100	33,272.9	6.550	4636.9	2.510	0.749	5506.5	2.347	0.993	7970.0	2.080	1.336

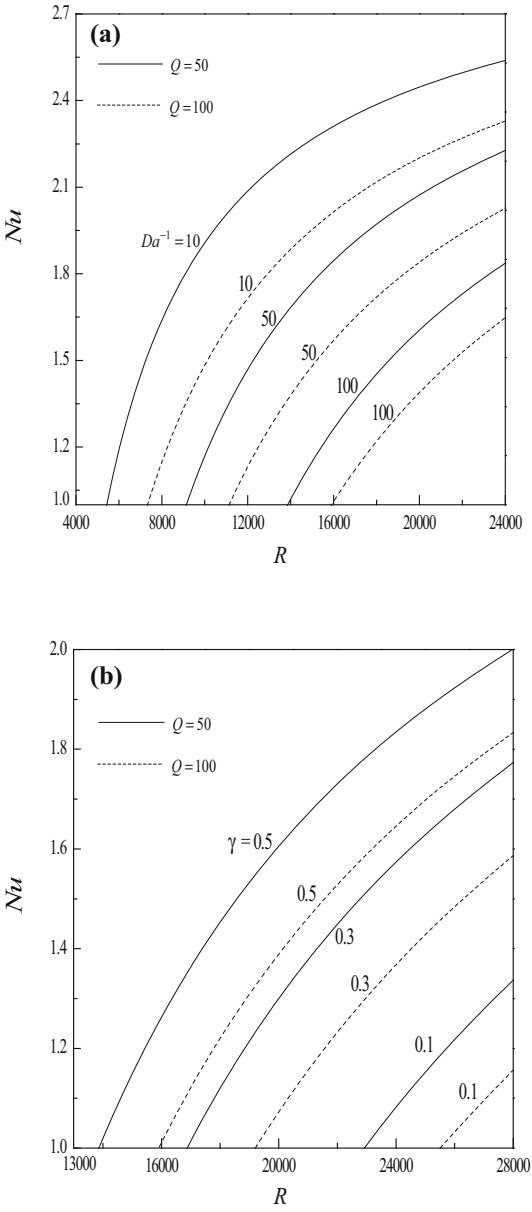

Fig. 11 Variation of Nu with R for different values of **a** Da^{-1} with $\tau = 2$, $\gamma = 0.5$, and $H = 100$ and **b** γ with $\tau = 2$, $Da^{-1} = 100$ and $H = 100$

oscillatory convection at moderate and higher values of H but at lower values of H, the curves of R_c for different α coalesce. In addition, it is seen that oscillatory convection is preferred to stationary convection for values of $\alpha \leq 1$ and beyond which the stationary convection is found to be a preferred mode of instability. The critical wave number for different values of α coalesces at smaller values of H while it increases with α with increasing H (Fig. 8b).

Figure 9a, b, respectively demonstrate the effect of Prandtl number Pr on the variation of R_c and a_c as a function of $\log_{10} H$ for $Da^{-1} = 100$, $Q = 100$, $\tau = 0.25$, $\gamma = 0.5$

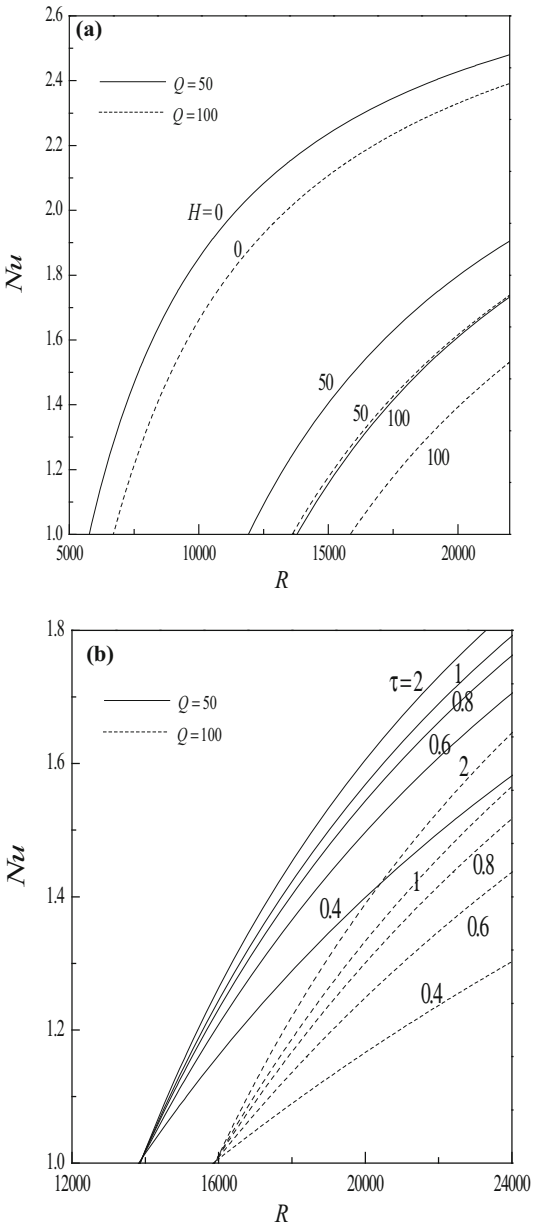

Fig. 12 Variation of Nu with R for different values of **a** H with $\tau = 2$, $\gamma = 0.5$, and $Da^{-1} = 100$ and **b** τ with $\gamma = 0.5$, $Da^{-1} = 100$ and $H = 100$

and $\alpha = 0.01$. Although increase in the value of Prandtl number is to advance the onset of convection, it is observed that its effect is insignificant once Pr exceeds the value unity (Fig. 9a). The critical wave number exhibits an increasing trend with Pr (Fig. 9b).

Since the strength of magnetic field alters significantly the nature of preferred mode of instability, the variation of critical Rayleigh number R_c with Q for different values of τ with $Da^{-1} = 25$, $\gamma = 0.5$, $\alpha = 0.01$ and $Pr = 1$ is shown explicitly in Fig. 10 for two values of $H = 0$ and 25. From the figure it is clear that the threshold value of Q (the value above

which oscillatory convection is preferred) increases with increasing τ in both LTE ($H = 0$) and LTNE ($H = 25$) cases. Further, the threshold values are lower for $H = 25$ compared to $H = 0$.

To know the occurrence of subcritical and supercritical bifurcations, the values of R^s obtained from Eq. (21) and $R^f_{\min}$ (minimum value of R^f obtained with respect to the amplitude A^2) obtained from Eq. (44) for different values of wave number and other physical parameters are tabulated in Table 3. It is observed that the results obtained for the case of nonporous domain ($Da^{-1} = 0 = H$) coincide with those of Knobloch et al. [7]. The critical value of stationary Rayleigh number (computed with respect to wave number) and the finite amplitude Rayleigh number (computed with respect to both wave number and amplitude) are denoted by R^s_c and R^f_c, respectively. To know the occurrence of subcritical instability the values of R^s_c and R^f_c obtained for $Q = 1000$, $\gamma = 0.5$, $Da^{-1} = 20$ and for several values of H are tabulated in Table 4. The results reveal that $R^f_c < R^s_c$ indicating the existence of subcritical instability for the chosen values of physical parameters. Besides, higher the critical wave number (narrow cells) for linear theory compared to nonlinear theory.

The vigor of convection is measured by the heat transfer across the porous layer and is calculated in terms of Nusselt number Nu. The variation of Nusselt number with Rayleigh number is shown in Figs. 11a, b and 12a, b for different values of physical parameters. It is seen that the Nusselt number increases with an increase in the value of Rayleigh number. Figure 11a, b, respectively show the variation of Da^{-1} (with $H = 100$, $\tau = 2$ and $\gamma = 0.5$) and γ (with $H = 100$, $\tau = 2$ and $Da^{-1} = 100$) on the Nusselt number for two values of Chandrasekhar number $Q = 50$ and 100. For the parametric values chosen, increasing Da^{-1} is to decrease the Nusselt number and hence its effect is to reduce the heat transfer, while increasing γ shows an opposite behavior on the heat transfer. Increasing the value of Q is to decrease the heat transport as it has a stabilizing effect on the onset of convection. The effect of increasing inter-phase heat transfer coefficient H is to lower the values of Nusselt number reiterating their stabilizing influence on the system (Fig. 12a). Increasing the value of τ is to increase the heat transport (Fig. 12b).

6 Conclusions

Magnetoconvection in a layer of Brinkman porous medium was investigated by performing both linear and weakly nonlinear stability analyses using a LTNE model. In the linear stability analysis, condition for the occurrence of stationary and oscillatory convection is obtained. The magnetic field has stabilizing effect on both stationary and oscillatory convection. Depending on the choice of parametric values, it is observed that exceeding certain value in the ratio of magnetic diffusivity to thermal diffusivity, Prandtl number and the ratio of fluid to solid thermal conductivities alters the preferred mode of instability from oscillatory to steady convection. However, stationary convection is always found to be the preferred mode of instability if the ratio of magnetic diffusivity to thermal diffusivity is greater than unity. The results also indicate that the threshold value of Chandrasekhar number (above which the preferred mode of instability is oscillatory convection) decreases for LTNE case compared to LTE case. The effect of increasing Chandrasekhar number is to decrease the size of convection cells. Also, the variation in the critical wave number with Chandrasekhar number in the stationary case is found to be dominant when compared to oscillatory case. Besides, the results obtained from the asymptotic analysis for small and large values of inter-phase heat transfer coefficient agree well with those obtained exactly. The weakly nonlinear stability

analysis carried out reveals the occurrence of subcritical instability for the choices of physical parameters. Heat transport is calculated in terms of Nusselt number. The magnetic field, inverse Darcy number and the inter-phase heat transfer coefficient have a retarding effect on heat transfer, while the porosity modified conductivity ratio and the ratio of magnetic to the thermal diffusivity have enhancing effect on heat transfer.

Acknowledgments The authors (ALM) and (MR) wish to thank their respective Principals of their colleges for encouragement. The authors thank the reviewers for their useful suggestions.

References

1. Thompson, W.B.: Thermal convection in a magnetic field. Phil. Mag. **42**, 1417–1432 (1951)
2. Chandrasekhar, S.: Hydrodynamic and Hydromagnetic Stability. Oxford University Press, London (1961)
3. Busse, F.H.: Nonlinear interaction of magnetic field and convection. J. Fluid Mech. **71**, 193–206 (1975)
4. Rudraiah, N.: Nonlinear interaction of magnetic field and convection in three dimensional motion. Pub. Astron. Soc. Japan **33**, 720–721 (1981)
5. Weiss, N.O.: Convection in an imposed magnetic field, part I. The development of nonlinear convection. J. Fluid Mech. **108**, 247–272 (1981)
6. Weiss, N.O.: Convection in an imposed magnetic field, part II. The dynamical regime. J. Fluid Mech. **108**, 273–289 (1981)
7. Knobloch, E., Weiss, N.O., Da Costa, L.N.: Oscillatory and steady convections in a magnetic field. J. Fluid Mech. **113**, 153–186 (1981)
8. Proctor, M.R.E., Weiss, N.O.: Magnetoconvection. Rep. Prog. Phys. **45**(11), 1317–1379 (1982)
9. Harfash, A.J., Straughan, B.: Magnetic effect on instability and nonlinear stability in a reacting fluid. Meccanica **47**, 1849–1857 (2012)
10. Makinde, O.D.: Magneto-hydromagnetic stability of plane-Poiseuille flow using multi-deck asymptotic technique. Math. Comput. Model. **37**, 251–259 (2003)
11. Makinde, O.D., Mhone, P.Y.: Temporal stability of small disturbances in MHD Jeffery–Hamel flows. Comput. Math. Appl. **53**, 128–136 (2007)
12. Wallace, W.E., Pierce, C.I., Sawyer, W.K.: Experiments on the flow of mercury in porous media in a transverse magnetic field. Bureau of Mines, Rep. No. RI-7259-PB-184327 (1969)
13. Rudraiah, N.: Laminar free convection flow of an electrically conducting fluid from an inclined isothermal plate. Israel J. Tech. **10**, 437–441 (1972)
14. Rudraiah, N., Vortmeyer, D.: Stability of finite-amplitude and overstable convection of a conducting fluid through porous bed. Warme Und Stoffubern. **11**, 241–254 (1978)
15. Rudraiah, N.: Linear and non-linear magnetoconvection in a porous medium. Proc. Ind. Acad. Sci. **93**, 117–135 (1984)
16. Raptis, A., Vlahos, J.: Unsteady hydromagnetic free convection flow through a porous medium. Lett. Heat Mass Trans. **9**, 59–64 (1982)
17. Raptis, A., Tzivanidis, G.: Hydromagnetic free convection flow through a porous medium between two parallel plates. Phys. Lett. A **90**, 288–289 (1982)
18. Takhar, H.S., Ram, P.C.: Effects of hall current on hydromagnetic free-convective flow through a porous medium. Astro. Space Sci. **192**, 45–51 (1992)
19. Bergman, M.I., Fearn, D.R.: Chimneys on the earth's inner–outer core boundary? Geo. Res. Lett. **21**, 477–480 (1994)
20. Alchaar, S., Vasseur, P., Bilgen, E.: Effects of a magnetic field on the onset of convection in a porous medium. Int. J. Heat Mass Trans. **30**, 259–267 (1995)
21. Bergman, M.I., Fearn, D.R., Bloxham, J.: Suppression of channel convection in solidifying Pb–Sn Alloys via an applied magnetic field. Metall. Mat. Trans. A **30**, 1809–1815 (1999)
22. Bhadauria, B.S.: Combined effect of temperature modulation and magnetic field on the onset of convection in an electrically conducting-fluid-saturated porous medium. ASME J. Heat Trans **130**, 052601–052609 (2008)
23. Muddamallappa, M.S., Bhatta, D., Riahi, D.N.: Numerical investigation on marginal stability and convection with and without magnetic field in a mushy layer. Trans. Porous Med. **79**, 301–317 (2009)
24. Bhatta, D., Muddamallappa, M.S., Riahi, D.N.: On Perturbation and marginal stability analysis of magnetoconvection in active mushy layer. Trans. Porous Med. **82**, 385–399 (2010)
25. Nield, D.A.: Impracticality of MHD convection in a porous medium. Trans. Porous Med. **73**, 379–380 (2008)

26. Riahi, D.N.: On Magneto convection in a mushy layer. Trans. Porous Med. **89**, 285–286 (2011)
27. Alzami, B., Vafai, K.: Analysis of variants within the porous media transport models. ASME J. Heat Trans. **122**, 303–326 (2000)
28. Straughan, B.: Global nonlinear stability in porous convection with a thermal non-equilibrium model. Proc. R. Soc. A **462**, 409–418 (2004)
29. Malashetty, M.S., Shivakumara, I.S., Kulkarni, S.: The onset of Lapwood–Brinkman convection using a thermal non-equilibrium model. Int. J. Heat Mass Trans. **48**, 1155–1163 (2005)
30. Nield, D.A., Bejan, A.: Convection in Porous Media, 3rd edn. Springer, New York (2006)
31. Srivastava, A.K., Bhadauria, B.S., Kumar, J.: Magnetoconvection in an anisotropic porous layer using thermal non-equilibrium model. Spl. Topics Rev. Porous Med. **2**, 1–10 (2011)
32. Shivakumara, I.S., Lee, J., Ravisha, M., Gangadhara Reddy, R.: The onset of Brinkman ferroconvection using a thermal non-equilibrium model. Int. J. Heat Mass Trans. **54**, 2116–2125 (2011)
33. Shivakumara, I.S., Lee, J., Ravisha, M., Gangadhara Reddy, R.: Effects of MFD viscosity and LTNE on the onset of ferromagnetic convection in a porous medium. Int. J. Heat Mass Trans. **54**, 2630–2641 (2011)
34. Cowling, T.G.: Magnetohydrodynamics. Adam Hilger Ltd., Bristol (1976)